

Regularized Dual-Channel Algorithm for the Retrieval of Soil Moisture and Vegetation Optical Depth From SMAP Measurements

Julian Chaubell , Simon Yueh , *Fellow, IEEE*, R. Scott Dunbar, Andreas Colliander , *Senior Member, IEEE*, Dara Entekhabi , *Fellow, IEEE*, Steven K. Chan, *Senior Member, IEEE*, Fan Chen , Xiaolan Xu , Rajat Bindlish , *Senior Member, IEEE*, Peggy O'Neill, *Fellow, IEEE*, Jun Asanuma, Aaron A. Berg , David D. Bosch , Todd Caldwell , Michael H. Cosh, *Senior Member, IEEE*, Chandra Holifield Collins, Karsten H. Jensen, Jose Martínez-Fernández, Mark Seyfried, Patrick J. Starks, Zhongbo Su, Marc Thibeault , and Jeffrey P. Walker 

Abstract—In August 2020, soil moisture active passive (SMAP) released a new version of its soil moisture and vegetation optical depth (VOD) retrieval products. In this article, we review the methodology followed by the SMAP regularized dual-channel retrieval algorithm. We show that the new implementation generates SM retrievals that not only satisfy the SMAP accuracy requirements, but also show a performance comparable to the single-channel algorithm that uses the V polarized brightness temperature. Due to a lack of *in situ* measurements we cannot evaluate the accuracy of the VOD. In this article, we show analyses with the intention of providing an understanding of the VOD product. We compare the VOD results with those from SMOS. We also study the relation of the SMAP VOD with two vegetation parameters: tree height and biomass.

Index Terms—Dual-channel algorithm, soil moisture active passive (SMAP), soil moisture (SM) retrieval, vegetation optical depth (VOD) retrieval.

I. INTRODUCTION

THE soil moisture active passive (SMAP) mission was designed to acquire and combine L -band radar and radiometer measurements for the estimation of soil moisture (SM) with an average unbiased root-mean square error (ubRMSE) of no more than $0.04 \text{ m}^3/\text{m}^3$ volumetric accuracy in the top 5 cm of soil for vegetation with water content of less than $5 \text{ kg}/\text{m}^2$ [1], [2]. SMAP released new versions of its SM and vegetation optical depth (VOD) products in August 2020 (version 4 for the L2/3_SM_P_E product and version 7 for the L2/3_SM_P).

The new implementation of the dual channel algorithm (DCA), which uses the two polarized brightness temperature measurements (H and V), generates SM retrievals, not only

satisfying the SMAP accuracy requirements, but also showing a performance comparable to the single-channel algorithm that uses the V polarized brightness temperature (SCA- V) [2], [3], [4].

While the accuracy of the DCA SM can be evaluated by comparison with *in situ* data, the lack of VOD *in situ* data raises concerns about the accuracy of the VOD product. Although the SMAP mission does not have a requirement for the accuracy of the retrieved VOD, it is of great value for the SMAP team and the science community in general since it provides critical information about the water content of the aboveground biomass and its seasonal variations. In order to understand the performance of the VOD product, it is common to compare it to similar products from other missions and to look at it in relation to other vegetation parameters such as tree height and biomass.

Recent efforts to retrieve SM and VOD from SMAP L -band brightness temperature data have resulted in significant progress [5]. Konings *et al.* [5] uses a multitemporal DCA (MT-DCA), which assumes that VOD changes more slowly than SM and can be assumed to be almost constant between every two consecutive overpasses. In addition, the MT-DCA approach allows for the retrieval of a single temporally constant value of the scattering albedo per pixel. The soil moisture and ocean salinity (SMOS) mission [6], produces simultaneous retrievals of SM and VOD based on angular information in its V - and H -pol brightness temperature products. Its L -band VOD retrievals have been analyzed by several authors [7]–[9]. SMOS-IC [10] presented an alternative approach to the retrieval of the SM and VOD but is still using angular brightness temperature information.

In this article, we detail the methodology for the DCA implementation in Section II. In Section III we present results of retrieved SM over core validation sites (CVSs) [4], [19]–[30], and the sparse network (SP) [17], [18]. We also present VOD results in Section III. In section IV we compare the SMAP VOD with the vegetation parameters, including tree height and biomass. In Section V, we compare the SMAP VOD results with those obtained by SMOS.

Manuscript received June 4, 2021; revised August 17, 2021; accepted October 15, 2021. Date of publication October 29, 2021; date of current version December 22, 2021. This work was supported by the Jet Propulsion Laboratory, California Institute of Technology under a contract with the National Aeronautics and Space Administration. (*Corresponding author: Julian Chaubell.*)

Please see the Acknowledgment section of this article for the author affiliations. Digital Object Identifier 10.1109/JSTARS.2021.3123932

II. REGULARIZED DUAL-CHANNEL ALGORITHM

The newly implemented DCA simultaneously retrieves the SM and VOD (τ_θ) by minimizing the cost function

$$F_D(\text{SM}, \tau_\theta) = [\text{TB}_V^{\text{sim}}(\text{SM}, \tau_\theta) - \text{TB}_V^{\text{obs}}]^2 + [\text{TB}_H^{\text{sim}}(\text{SM}, \tau_\theta) - \text{TB}_H^{\text{obs}}]^2 + \lambda^2(\tau_\theta - \tau^*)^2 \quad (1)$$

where TB_V^{sim} is the V -polarized simulated brightness temperature and TB_H^{sim} is the H -polarized simulated brightness temperature, λ is a regularization parameter, and τ^* an initial expected VOD value.

To simulate the L -band emission of the soil-vegetation system the SMAP team uses the zero-order approximation of the radiative transfer equations, known as the τ - ω emission model [10]. The brightness temperature equation, which includes emission components from the soil and the overlying vegetation canopy, is given by

$$\begin{aligned} \text{TB}_p^{\text{sim}} &= T_s e_p \exp(-\tau_p \sec \theta) + T_c (1 - \omega_p) \\ &\quad [1 - \exp(-\tau_p \sec \theta)] \\ &\quad [1 + r_p \exp(-\tau_p \sec \theta)] \end{aligned} \quad (2)$$

where the subscript p refers to polarization (V or H), T_s is the soil effective temperature, T_c is the vegetation temperature, τ_p is the nadir vegetation opacity, ω_p is the vegetation effective scattering albedo, r_p is the rough soil reflectivity, e_p is the rough soil emissivity and θ is the incidence angle.

The surface roughness reflectivity is modeled by

$$r_p(\theta) = [(1 - Q)r_p^*(\theta) + Qr_q^*(\theta)] e^{-h \cos^N(\theta)} \quad (3)$$

where Q (polarization decoupling factor which is related to h by the linear relation $Q = 0.1771 h$), h , and N are the roughness parameters and $r_p^*(\theta)$ is the Fresnel reflectivity of the smooth surface where the index p and q (q opposite to p) account for the polarization V or H . The baseline SMAP implementation of the retrieval algorithms assumes that in (2) $T_s = T_c$ at the early morning descending overpass and that $\omega_p = \omega$ and $\tau_p = \tau$ are polarization independent to reduce the number of algorithm parameters [2]. Note that in (1) τ_θ is related to the nadir vegetation opacity by $\tau_\theta = \tau \sec \theta$.

The implementation of (1)–(3) requires that several parameters need to be assumed: *a priori* value of the scattering albedo based on land cover, roughness parameters as detailed in [3], effective soil temperature, clay fraction to determine the soil dielectric constant, as well as the regularization parameters τ^* and λ [2].

A. Selection of Parameter λ

The retrieval of VOD through the DCA algorithm with $\lambda = 0$ (MDCA, modified DCA [3]) produces VOD results with high variability in the temporal dimension as shown in Fig. 1(a) (blue curve) and also in the spatial dimension. Fig. 1(a) displays an example of the MDCA climatology at the Monte Buey CVS. It also shows the seven-day average and the VOD based on Normalized Difference Vegetation Index (NDVI) climatology from the moderate-resolution imaging spectroradiometer (MODIS).

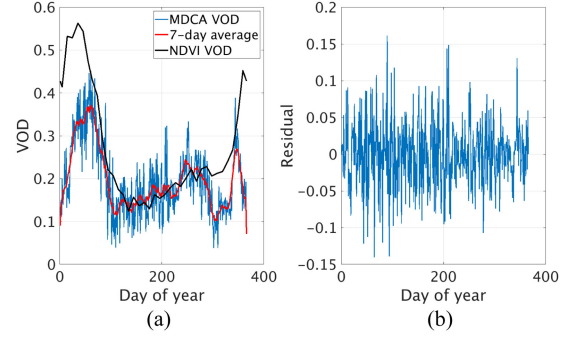


Fig. 1. Climatology over Monte Buey (lat -32.91, lon -62.51) SMAP CVS. (a) Residual obtained by subtracting the 7-day average and the MDCA climatology. (b) Residual with seasonal variation removed is used to compute $\lambda = 1/\sigma$. The NDVI climatology shown on the (a) (black curve) shows the selected initial guess over that CVS.

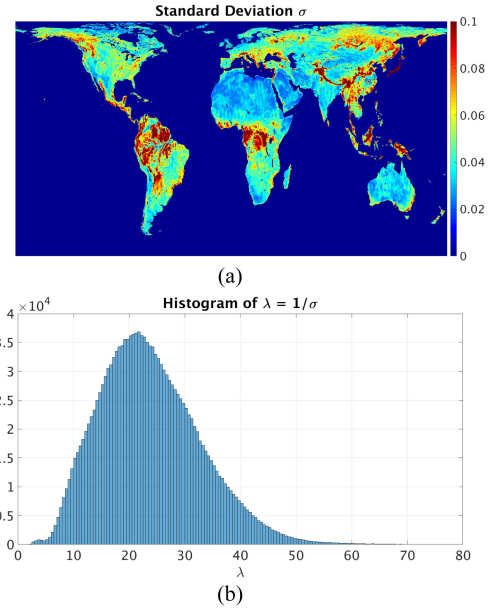


Fig. 2. Global map of σ (top) from the residuals as in Fig. 1. At the bottom the histogram of the corresponding λ . The histogram shows the peak value at $\lambda \approx 20$.

The selection of λ determines how much the residual noise [see Fig. 1(b)] will be suppressed and how much freedom the optimization algorithm will have to converge to a solution of VOD apart from the expected value τ^* . Indeed, the value of $\lambda = 0$ means no regularization and very high values of λ will force the retrieval of VOD to converge to τ^* .

To select potential candidates of λ we considered five years (April 4, 2015–March 31, 2020) of MDCA VOD data for each 9km EASE-2 (equal area scalable earth grid version 2) grid cell and computed its daily climatology, Fig. 1(a). To remove the seasonal variation, we computed a seven-day average [red curve in Fig. 1(a)] which is subtracted from the MDCA climatology resulting in the residual shown in Fig. 1(b). We used the standard deviation (σ) of the residual to determine the amount of regularization needed and defined λ as $1/\sigma$. Fig. 2 displays a global map of σ (top) and the histogram of the corresponding

TABLE I
ACRONYMS SUMMARY

Algorithm	Description
DCA	Dual-channel algorithm. It uses the two polarized brightness temperature measurements (H and V) to simultaneously retrieve SM and VOD. General algorithm name.
MDCA	Modified dual-channel algorithm [3]. This implementation includes changes in the roughness reflectivity model with respect to the original SMAP DCA implementation. No regularization is applied.
RDCA	Modified dual-channel algorithm with regularization. Regularization parameter $\lambda = 20$ globally. In August 2020 we renamed the modified dual-channel algorithm to DCA which corresponds to the RDCA configuration.
RDCA- λ	Modified dual-channel algorithm with regularization. Regularization parameter varying globally.

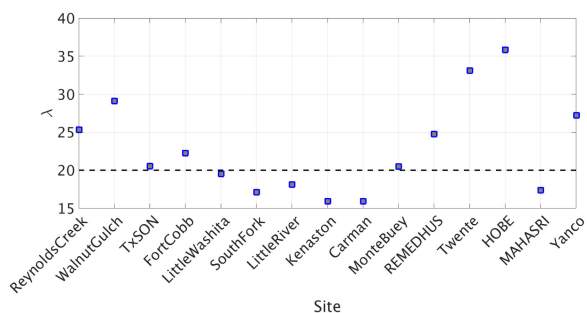


Fig. 3. Values of λ at each CVS used to evaluate RDCA- λ .

TABLE II
RDCA, RDCA- λ PERFORMANCE COMPARISON

Alg.	ubRMSE	RMSE	Bias	Corr.	MaBias
RDCA	0.36	0.46	-0.010	0.819	0.037
RDCA- λ	0.36	0.47	-0.009	0.821	0.038

Performance analysis of SM retrievals over SMAP CVS for $\lambda = 20$ (RDCA) or the corresponding local values (RDCA- λ), as shown in Fig. 2.

λ (bottom). Fig. 2 shows that σ varies across the globe and that the histogram peaks at $\lambda \sim 20$.

We evaluated the performance of the SM retrievals compared to *in situ* SM data from 15 SMAP CVS by setting $\lambda = 20$ fixed over all the sites and also using the local values of lambda over each CVS. Fig. 3 displays the values of lambda for each CVS. In what follows we will refer to RDCA for the regularized DCA algorithm with regularization parameter $\lambda = 20$ and RDCA- λ for the regularized DCA algorithm with λ changing spatially.

Table I gives the acronyms used to differentiate the different DCA implementations.

Table II gives the algorithm performance metrics for SM retrievals. The metrics are the average of those at each CVS. The metrics show that even though a nonzero lambda is crucial to get good performance by the DCA algorithm, the selection of the values of λ is not relevant as long as λ is allowed to vary locally about the value $\lambda = 20$. For this reason and considering the ease of the operational implementation we decided to set $\lambda = 20$ globally.

B. Selection of the Initial Guess τ^*

As an initial guess τ^* , an estimate of VOD based on NDVI climatology was selected [2]. This selection aroused concerns regarding how the seasonal behavior of the RDCA VOD would be affected.

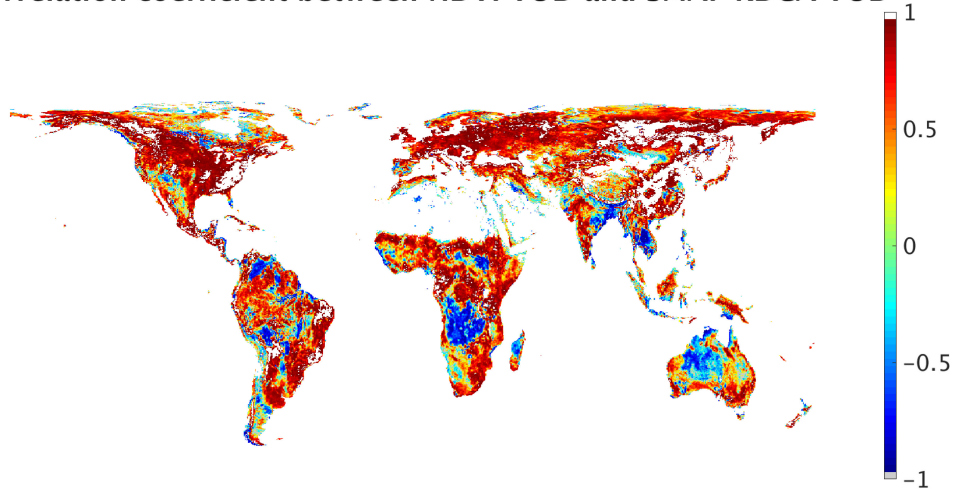
To address this, we compared the Pearson correlation of the daily climatology of RDCA VOD with daily climatology of NDVI VOD [see Fig. 4(a)] and daily climatology of MDCA VOD [see Fig. 4(b)]. The figure shows that while the correlation between RDCA VOD and the NDVI VOD is moderate (mean value of 0.51 and standard deviation of 0.51), there is a high correlation globally between RDCA VOD and MDCA VOD (mean value of 0.76 and standard deviation of 0.25) which is an indication that RDCA VOD follows the MDCA VOD seasonal variation more consistently than the seasonal variation of the NDVI VOD. We also looked into the time difference (in days) between the NDVI τ^* peak location (see Fig. 1, black curve) and the peak location of the RDCA VOD climatology (see Fig. 1, red curve) and similarly for MDCA VOD and RDCA VOD. Fig. 5 displays the histograms of differences. We can see that while the differences are widespread for NDVI τ^* minus RDCA VOD, for RDCA VOD – minus MDCA VOD most of the values concentrate around zero. This is another indication that both MDCA VOD and RDCA VOD reach their maximum value at approximately the same time. These two tests suggest that in general the use of the NDVI τ^* does not affect the seasonal variation of the MDCA VOD significantly.

III. ASSESSMENT

The SMAP mission validates the accuracy of the retrieved SM using several sources of information [15]. Among them are CVS which provide the ground-based data in a timely manner to the SMAP project, and SPs, such as the USDA soil climate analysis network [16], the NOAA Climate Research Network [17] and the Oklahoma Mesonet [18].

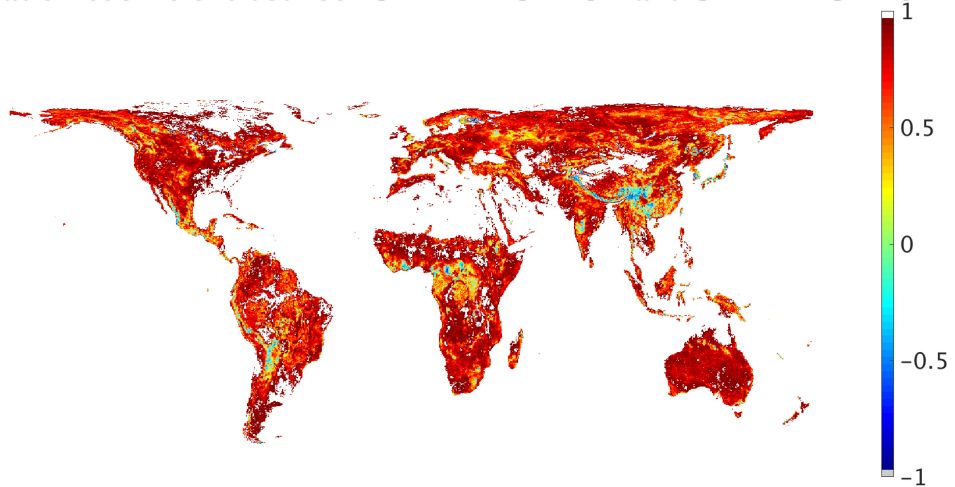
Table III gives how the SCA-V, MDCA, and RDCA SM retrievals compare at the CVS. We can see that a significant improvement has been reached by the implementation of the regularization term in the DCA algorithm. The table also shows that the RDCA and SCA-V are statistically similar.

Correlation coefficient between NDVI VOD and SMAP RDCA VOD



(a)

Correlation coefficient between SMAP MDCA VOD and SMAP RDCA VOD



(b)

Fig. 4. Correlation map between NDVI VOD and RDCA VOD. (a) Between RDCA VOD and MDCA VOD (b) Grey areas indicate pixel with p -values > 0.05 . White areas indicate not available data.

TABLE III
ASSESSMENT OF SM RETRIEVALS OVER CVS

Descending												
Algorithm	MDCA				SCA-V				RDCA			
	ubRMSE	Bias	RMSE	R	ubRMSE	Bias	RMSE	R	ubRMSE	Bias	RMSE	R
Mean	0.041	-0.006	0.052	0.762	0.038	-0.006	0.048	0.814	0.036	-0.009	0.045	0.815
Ascending												
Algorithm	MDCA				SCA-V				RDCA			
	ubRMSE	Bias	RMSE	R	ubRMSE	Bias	RMSE	R	ubRMSE	Bias	RMSE	R
Mean	0.041	-0.006	0.052	0.762	0.037	-0.008	0.048	0.807	0.036	-0.013	0.045	0.787

CVS assessment of soil moisture retrievals. 5 years (04/01/2015-03/31/2020) of data were used to compare the accuracy of MDCA with SCA-V and RDCA. We display the averaged RMSE(m^3/m^3), ubRMSE(m^3/m^3), Bias(m^3/m^3) and correlation (R) over 15 SMAP CVS.

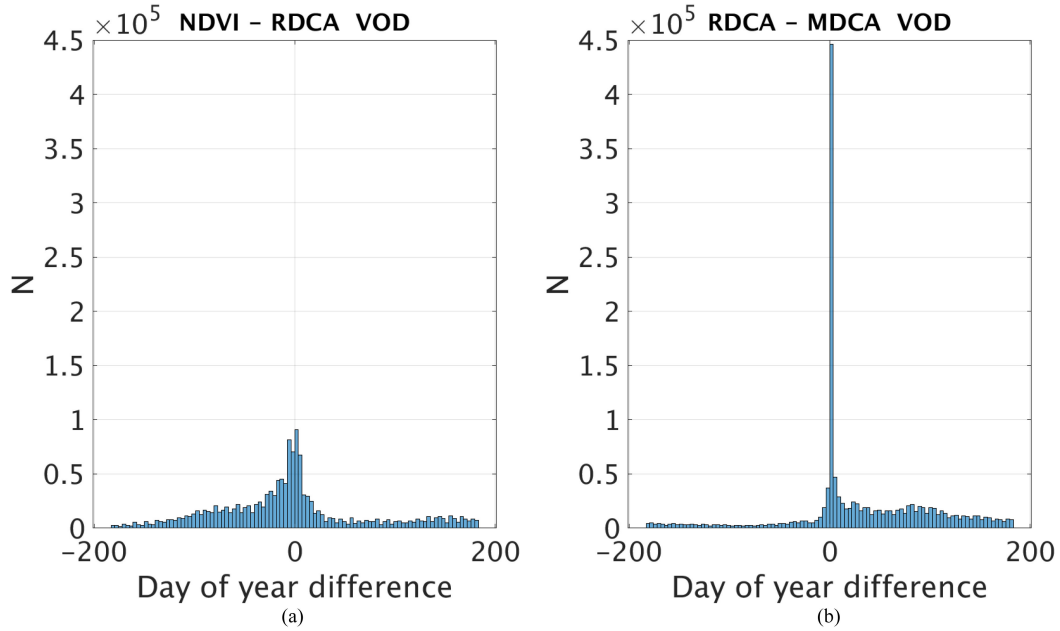


Fig. 5. Time differences of vegetation peak occurrence in days. (a) Difference between NDVI VOD and SMAP RDCA VOD. (b) Difference between SMAP RDCA VOD and MDCA VOD.

TABLE IV
ASSESSMENT OF SM RETRIEVALS OVER SP

Descending	MDCA				SCA-V				RDCA			
Algorithm	ubRMSE	Bias	RMSE	R	ubRMSE	Bias	RMSE	R	ubRMSE	Bias	RMSE	R
Mean	0.049	0.008	0.070	0.660	0.048	-0.001	0.069	0.659	0.047	0.006	0.070	0.667
Ascending	MDCA				SCA-V				RDCA			
Algorithm	ubRMSE	Bias	RMSE	R	ubRMSE	Bias	RMSE	R	ubRMSE	Bias	RMSE	R
Mean	0.049	0.009	0.071	0.623	0.047	0.002	0.069	0.633	0.047	0.007	0.069	0.639

SP assessment of SM retrieval. A total of five years (January 4, 2015–March 31, 2020) of data were used to compare the accuracy of MDCA (DCA with $\lambda = 0$) with SCA-V (single channel algorithm with V polarization measurement of brightness temperature) and RDCA (DCA with $\lambda = 20$). We display the averaged RMSE(m³/m³), ubRMSE(m³/m³), Bias(m³/m³), and correlation (R) over several land cover types.

Table IV gives the assessment report over the SPs using five years of SMAP SM data (January 4, 2015–March 31, 2020). The table compares the accuracy of MDCA, SCA-V and RDCA. We display ubRMSE, bias, and correlation (R) for several land cover types: evergreen needleleaf forest; open shrublands; woody savannas; savannas; grasslands; croplands; crop/natural vegetation mosaic; and Barren/Sparse. We observe again that SCA-V and RDCA present similar performance and that RDCA shows a significant improvement with respect to MDCA. A thorough analysis of the SMAP SM performance can be found in [4].

IV. SMAP VOD VERSUS TREE HEIGHT AND BIOMASS

In this section, we analyze the correlation between the SMAP RDCA VOD and two vegetation parameters: tree height in unit of meters (m) [13] and the aboveground biomass density of vegetation in units of Mg/ha [14]. Both sets of data were aggregated to the 9km EASE-2 to match the enhanced SMAP data, Fig. 6.

Fig. 7(a) displays the density plots of VOD versus tree height and Fig. 7 (b) and (c) displays VOD versus biomass. Fig. 7 also displays the mean values for several bins and the fitting curve. To compute the mean values, the data were binned by intervals of tree height of 1 m and the biomass by intervals of 10 Mg/ha.

There is clear linearity between SMAP RDCA VOD and tree height spatially for values of tree height less than 20 m and the relationship remains fairly linear up to tree heights of ~ 35 m/ the slope of the fitting curve is 0.033 and the offset is -0.06. The spatial correlation between SMAP RDCA VOD and the tree height map is $R = 0.81$ (strong).

The VOD versus biomass density plot [see Fig.7(b)] also shows linearity for values of biomass less than 90 Mg/ha. The VOD versus biomass (B) fitting curve for values of B between 0 and 90 Mg/ha is given by

$$\text{vod} = 0.004854 B + 0.2541. \quad (4)$$

For values of biomass greater than 90 Mg/ha and less than 150 Mg/ha the VOD stays almost constant, this could be caused

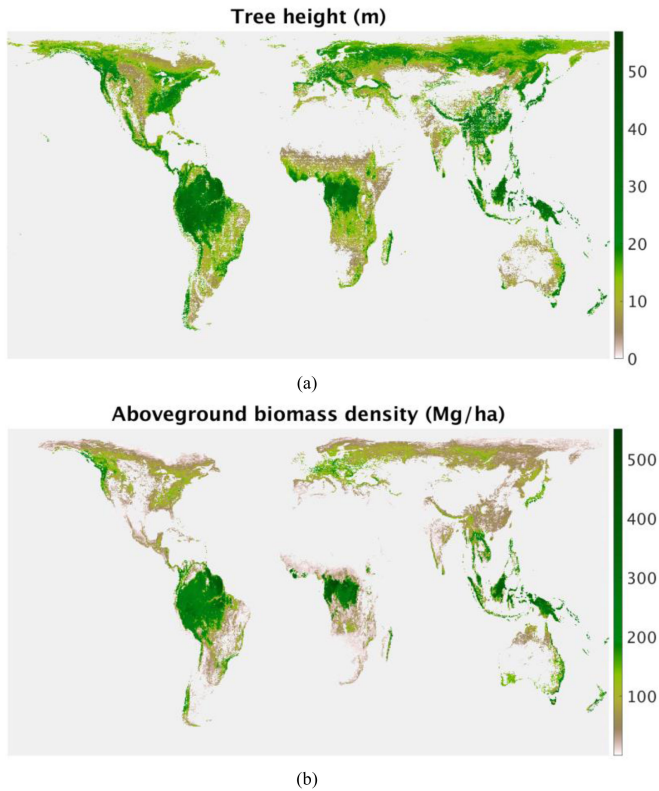


Fig. 6. (a) Tree height (meters). (b) Aboveground biomass density of vegetation in units of Mg/ha.

by a reduction in the amount of data points together with an increase in dispersion. Fig 7(c) shows that after B values of 150 Mg/ha the VOD starts increasing again and reaches saturation at about B values of 240 Mg/ha.

Heterogeneity of the grid pixel could be one of the factors causing the scatter in the density plots. The spatial correlation between the SMAP VOD and the biomass map is $R = 0.53$ (moderate).

V. SMAP RDCA VOD VERSUS SMOS VOD

The lack of VOD *in situ* data makes it difficult to evaluate the accuracy and performance of the SMAP RDCA VOD product. In order to understand the performance of the VOD product we compare the SMAP RDCA VOD product (L2_SM_P_E v4 [12]) with the SMOS Level 3 VOD.¹ For comparison, the SMAP RDCA VOD product was multiplied by $\cos(40^\circ)$ to match the SMOS VOD product at nadir.

Fig. 8 displays global maps of VOD. The SMAP data were aggregated to the 25 km EASE-2 grid to match the SMOS data. We observed that the SMOS VOD has higher values of VOD. In fact, the mean VOD and standard deviation for the SMOS are 0.42 and 0.28 respectively, while for SMAP, those values are 0.29 and 0.26, respectively. This difference in value may be caused by different levels of the roughness parameters used by the two missions. Table V gives the mean and standard deviation

for SMOS, SMAP, and the NDVI VOD by land cover type following the MODIS-based IGBP (International Geosphere Biosphere) classification. For the computation of the statistics, we considered only pixels with Gini–Simpson-Index (GSI) less than 0.1. The GSI is commonly used in ecology as a measure of degree of homogeneity, where $GSI = 0$ means total homogeneity and is computed as

$$GSI = 1 - \sum_{i=1}^n f_i^2 \quad (5)$$

where f_i is the fraction of the area covered by the i th land use classification and n is the number of land cover types. Table V gives that in general there is very good agreement between the magnitude of the SMAP RDCA VOD and the magnitude of the NDVI VOD. This is somehow expected due to the nature of the roughness parameter h implemented by the SMAP algorithm [3]. In the τ - ω emission model τ and h cannot be seen as parameter independent of each other and the magnitude of the selected h will affect the magnitude of the retrieved τ . Since the values of h are obtained by a DCA-type algorithm involving NDVI τ as an input, we expect to have retrieved values of τ of magnitude similar to the NDVI τ . However, since the values of h are temporal invariant, the seasonality variation of τ should not be affected.

Table V also gives that there is very good agreement with SMOS VOD over forested areas although SMOS data seem to have more variability. In fact, SMOS data seem to have more variability for all the land cover types except for Urban and built-up settings. For land cover types other than forest we observed significant discrepancies in the statistics between SMOS and SMAP RDCA VOD.

Fig. 9 displays the VOD differences for two consecutive years: 2015–2016 and 2016–2017. SMAP RDCA VOD tracks yearly changes in VOD unlike the NDVI VOD which is a ten-year climatology. The SMOS VOD product exhibits more variability than the SMAP RDCA VOD. SMAP RDCA VOD is smoother due to the use of NDVI VOD as regularization parameter τ^* . There are some similarities between SMOS and SMAP but also some discrepancies. For example, over Australia, in Fig. 9 (top row), the trends seem to agree although SMOS shows greater differences. On the other hand, in Fig. 9(bottom row) over the same region the trends are distinctly different except for a portion in the east-central part of the country. We also see discrepancies in Fig. 9 (top row) for the east coast of the United States.

Fig. 10 displays the Pearson correlation (R) between SMAP and SMOS VOD. The aggregated SMAP RDCA VOD and the SMOS VOD were averaged monthly, thus obtaining two data sets of dimensions (1388584,60) and then for each grid cell the temporal correlation was obtained. We observed that the correlation varies along the globe with a mean value of 0.344 (weak correlation) and standard deviation of 0.33. If we only consider correlation with p-values < 0.05 then the mean correlation value is 0.542 (moderate correlation) and the standard deviation is 0.26. It is noticeable that the correlation is mostly positive indicating a degree of agreement in trends.

¹[Online]. Available: ftp://ftp.ifremer.fr/Land_products/GRIDDED/L3SM

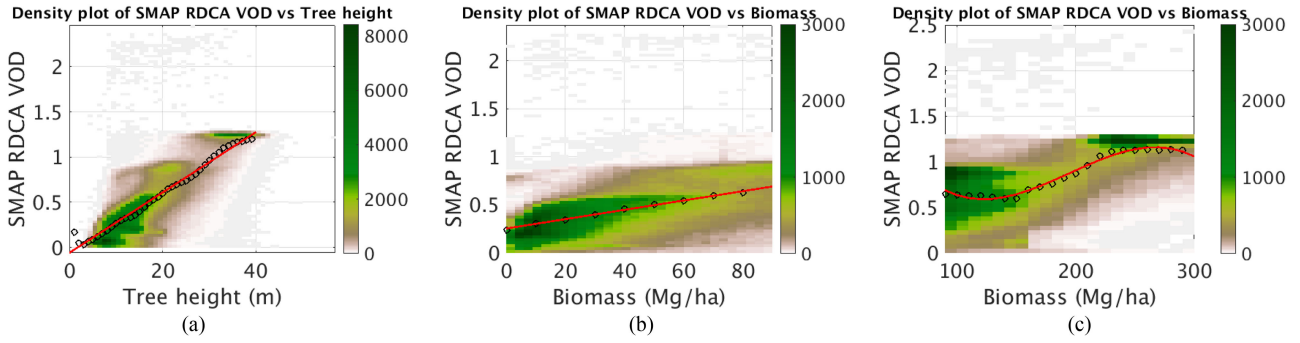


Fig. 7. Density plots and mean fitting curves. (a) SMAP RDCA VOD versus Tree height. (b) SMAP RDCA VOD versus Biomass for values of biomass less than 90 Mg/ha. (c) SMAP RDCA VOD versus Biomass for values of biomass greater than 90 Mg/ha and less than 300 Mg/ha.

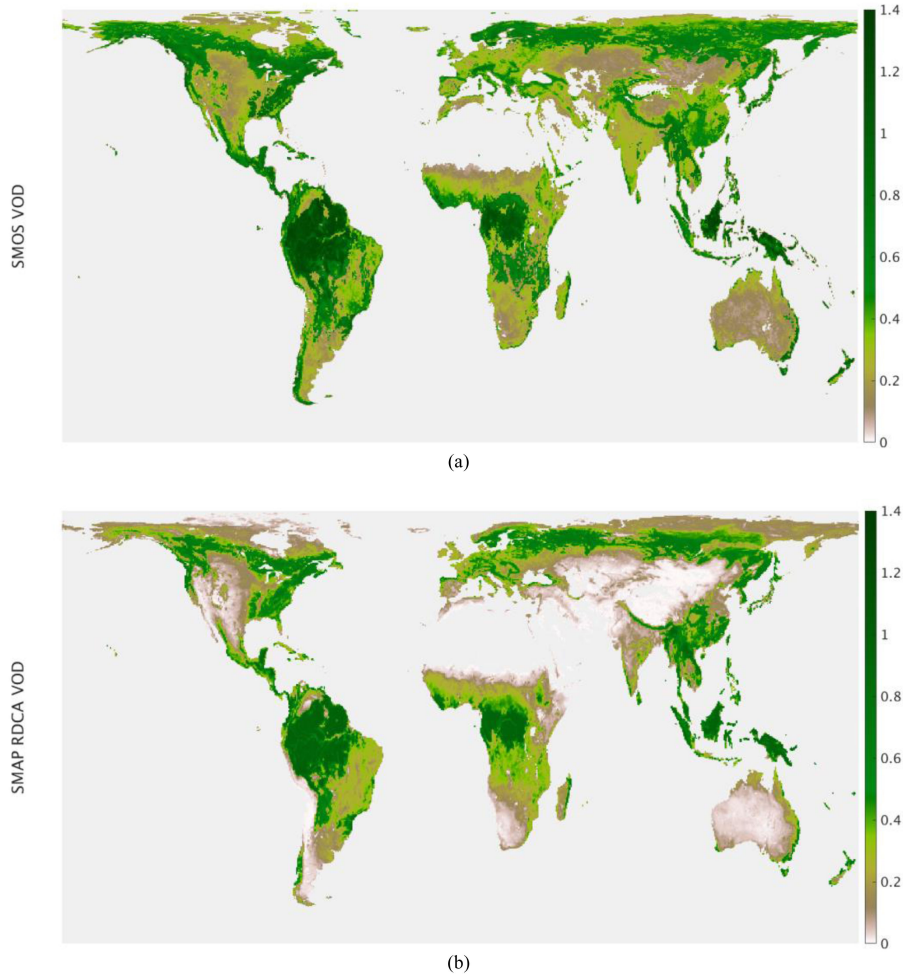


Fig. 8. Global maps of averaged SMOS VOD (a) and SMAP RDCA VOD (b) for five years of data (04/01/2015-03/31/2020).

Table VI gives the correlation by land cover types using only pixels with significant correlation, p -value < 0.05 . We observed mostly moderate correlation, with the exception of permanent wetlands (PW) where the correlation is strong and evergreen needle leaf forest (ENF), evergreen broadleaf forest (EBF), closed shrublands (CS) and barren/sparse (BS) where the correlation is weak. Fig. 11 displays the monthly average of VOD at five different regions. From top to bottom the regions are as follows.

- 1) Peruvian Amazonia [-4.5 -4 -75 -74.5], land cover type: Evergreen broadleaf forest. The SMOS-SMAP correlation is very weak $R = 0.148$ and p -value > 0.05 .
- 2) Angola [-12.5 -12 17 17.5], land cover type: Woody savannas. The SMOS-SMAP correlation is strong $R = 0.806$ and p -value < 0.05 .
- 3) South Fork, Iowa [42 42.5 -93.5 -93], land cover type: Croplands. The SMOS-SMAP correlation is strong $R = 0.873$ and p -value < 0.05 .

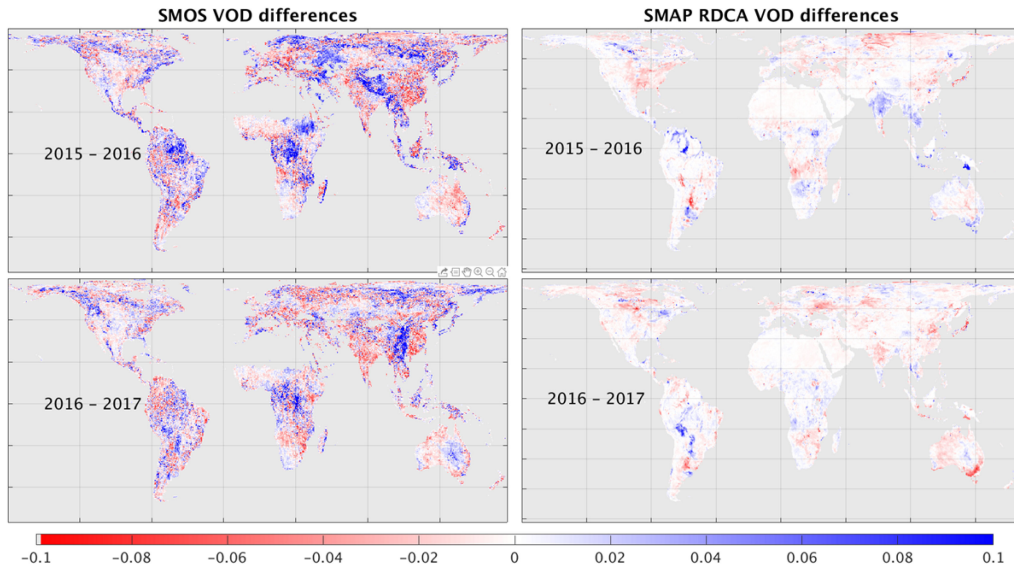


Fig. 9. VOD difference for two consecutive years. 2015–2016 on top and 2016–2017 on the bottom.

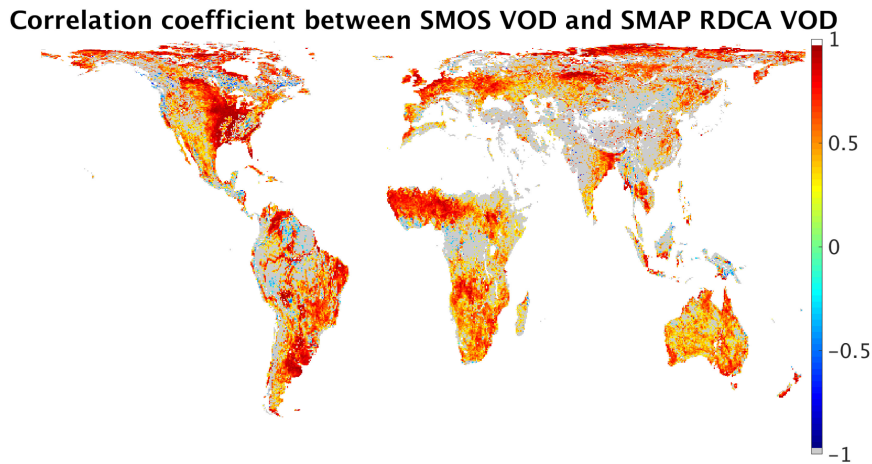


Fig. 10. Map of Pearson correlation between monthly averaged SMOS and SMAP RDCA VOD. Grey areas indicate pixel with p -values > 0.05 . White areas indicate not available data.

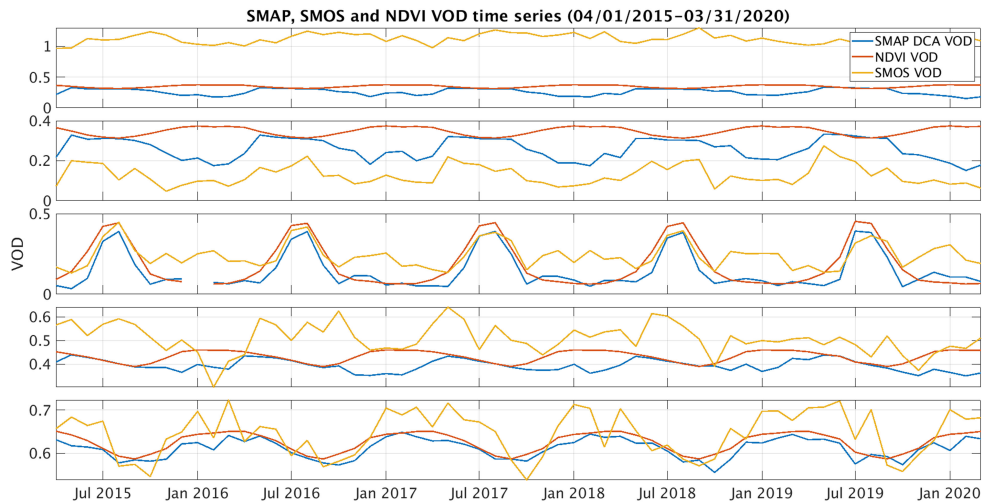


Fig. 11. Sixty months (January 4, 2015–March 31, 2020) of averaged VOD (SMAP, SMOS and NDVI) for five different regions. From top to bottom: Peruvian Amazonia; Angola; South Fork (Iowa); Zambia; and Chaco (Argentina).

TABLE V
SMAP AND SMOS STATISTICS COMPARISON BY LAND COVER TYPE

Land cover type	SMOS mean	SMAP mean	NDVI mean	SMOS std	SMAP std	NDVI std	N
Evergreen needleleaf forest	0.64	0.62	0.64	0.12	0.08	0.07	598
Evergreen broadleaf forest	1.08	0.91	0.93	0.20	0.07	0.05	12295
Deciduous needleleaf forest	0.54	0.44	0.45	0.10	0.02	0.02	762
Deciduous broadleaf forest	0.71	0.64	0.65	0.13	0.06	0.06	363
Mixed forest	0.64	0.66	0.67	0.12	0.08	0.04	2204
Closed shrublands	NaN	NaN	NaN	NaN	NaN	NaN	0
Open shrublands	0.24	0.07	0.07	0.14	0.06	0.05	16734
Woody savannas	0.54	0.37	0.42	0.18	0.05	0.04	3403
Savannas	0.31	0.24	0.26	0.12	0.05	0.05	4005
Grasslands	0.19	0.04	0.06	0.09	0.03	0.04	10900
Permanent wetlands	0.39	0.07	0.07	0.38	0.16	0.17	10
Croplands	0.25	0.12	0.18	0.06	0.05	0.04	4923
Urban and built-up	0.28	0.10	0.23	0.05	0.14	0.02	4
Crop/Natural vegetation mosaic	0.33	0.25	0.29	0.17	0.12	0.11	243
Snow and ice	0.33	0.04	0.03	0.27	0.04	0.05	17705
Barren/Sparsely vegetated	0.18	0.01	0.00	0.11	0.00	0.00	23565

Statistics of SMAP, SMOS, and NDVI VOD by land cover type classification. N represents the number of pixels involved in the computation. Pixels with GSI < 0.1 were considered.

TABLE VI
SMAP VS SMOS VOD CORRELATION BY LAND COVER

ENF	EBF	DNF	DBF	MF	CS	OS	WS	S	G	PW	C	UB	CNVM	SI	BS
0.306	0.363	0.531	0.472	0.503	0.300	0.543	0.511	0.576	0.566	0.723	0.631	0.582	0.620	0.605	0.340

SMAP RDCA VOD versus SMOS VOD monthly timeseries Pearson correlation by land cover types as defined by the IGBP land cover classification (land cover abbreviations from Table IV). The analysis was performed only for pixels with significant correlation p -value < 0.05.

- 4) Zambia [-14.5 -14 24 24.5], land cover type: Woody savannas. The SMOS-SMAP correlation is moderate $R = 0.435$ and p -value < 0.05.
- 5) Chaco, Argentina [-25.5 -25 -62.5 -62], land cover type: Deciduous broadleaf forest. The SMOS-SMAP correlation is strong $R = 0.747$ and p -value < 0.05.

We see that in all the cases the SMOS and SMAP have consistent trends while NDVI VOD trends only agree with SMAP and SMOS over Chaco and South Fork. There is a big difference in the VOD magnitude over the Peruvian Amazonia and very weak correlation caused by the low seasonal change of VOD combined with the differences in short term variability. The correlation is not significant according to the p -value (we consider a correlation to be significant if the p -value is < 0.05). We also observed that the SMOS VOD has more variability which may be the cause of low correlation in some locations, as can be seen in the Zambia case, Fig. 11 second from the bottom.

The spatial correlation between SMOS VOD and SMAP RDCA VOD as shown in Fig. 8 is $R = 0.83$ (strong).

VI. CONCLUSION

In this article, we have shown that the regularized DCA algorithm (RDCA along this article) implemented in the new release (R17) allows for an accurate retrieval of SM and a reliable VOD (τ). Indeed, we showed that the DCA SM not only satisfies the SMAP requirements but also showed accuracy levels comparable to the SMAP SCA-V baseline. We compared

the SMAP RDCA VOD with the SMOS VOD. We showed that even though there are differences in magnitude, they have, in general, consistent temporal behavior tracking seasonal changes and strong spatial correlation.

Comparison of the SMAP RDCA VOD with tree height showed strong correlation and a linear relation especially for tree height less than 20 m.

Comparison of the SMAP RDCA VOD with vegetation biomass showed moderate correlation. We also observed linear correlation for biomass less than 90 Mg/ha.

The magnitude of the SMAP RDCA VOD is comparable to the magnitude of the NDVI VOD due to the nature of the selection of the roughness parameter h . However, since the values of h are temporal invariant, the seasonality variation of the retrieved VOD should not be affected.

The application of temporal variant roughness parameter h should be explored for further improvement of the retrieved VOD.

ACKNOWLEDGMENT

This article is carried out by the Jet Propulsion Laboratory, California Institute of Technology, under a contract with the National Aeronautics and Space Administration. The SMOS Data were obtained from the ‘‘Centre Aval de Traitement des Donnees SMOS’’ (CATDS), operated for the ‘‘Centre National d’Etudes Spatiales’’ (CNES, France) by IFREMER (Brest, France). USDA is an equal opportunity provider and employer. The research described in this publication also included measurements

from the Long-Term Agroecosystem Research (LTAR) network. LTAR is supported by the U.S. Department of Agriculture. The University of Salamanca team involvement in this study was supported by the Spanish Ministry of Science and Innovation (projects ESP2017- 89463-C3-3-R and PID2020-114623RB-C33), the Castilla y León Government (projects SA112P20 and CLU-2018-04) and the European Regional Development Fund (ERDF). The authors would like to thank Heather McNairn of the Agriculture and Agri-Food Canada (AAFC) for her work managing the core validation sites Carman.

Authors' Affiliations

Julian Chaubell, Simon Yueh, R. Scott Dunbar, Andreas Colliander, Steven K. Chan, and Xiaolan Xu are with the Jet Propulsion Laboratory, California Institute of Technology, Pasadena, CA 91109 USA (e-mail: mario.j.chaubell@jpl.nasa.gov; simon.yueh@jpl.nasa.gov; roy.s.dunbar@jpl.nasa.gov; andreas.colliander@jpl.nasa.gov; stevents.k.chan@jpl.nasa.gov; xiaolan.xu@jpl.nasa.gov).

Dara Entekhabi is with the Massachusetts Institute of Technology, Cambridge, MA 02139 USA (e-mail: darae@mit.edu).

Fan Chen is with the SSAL Inc., Greenbelt, MD and USDA Agricultural Research Service, Beltsville, MD 20705 USA (e-mail: fan.chen@ars.usda.gov).

Rajat Bindlish and Peggy O'Neill are with the Goddard Space Flight Center, Greenbelt, MD 20771 USA (e-mail: rajat.bindlish@nasa.gov; peggy.e.oneill@nasa.gov).

Jun Asanuma is with the Center for Research in Isotopes and Environmental Dynamics, Tsukuba University, Tsukuba 305-8577, Japan (e-mail: asanuma@ied.tsukuba.ac.jp).

Aaron A. Berg is with the Department of Geography, Environment and Geomatics, University of Guelph, Guelph, ON N1G 2W1, Canada (e-mail: aberg@uoguelph.ca).

David D. Bosch is with the USDA Agricultural Research Service Southeast Watershed Research Laboratory, Tifton, GA 31794 USA (e-mail: david.bosch@usda.gov).

Todd Caldwell is with the University of Texas at Austin, Bureau of Economic Geology, Austin, TX 78758 USA (e-mail: tcaldwell@usgs.gov).

Michael H. Cosh is with the USDA Agricultural Research Service Beltsville Agricultural Research Center, Hydrology and Remote Sensing Laboratory, Beltsville, MD 20705 USA (e-mail: michael.cosh@usda.gov).

Chandra Hollifield Collins is with the USDA Agricultural Research Service Southwest Watershed Research, Southwest Watershed Research Center, Tucson, AZ 85719 USA (e-mail: chandra.hollifield@usda.gov).

Karsten H. Jensen is with the Department of Geosciences and Natural Resource Management, DK-1350 Copenhagen K, Denmark (e-mail: khj@ign.ku.dk).

Jose Martínez-Fernández is with the Instituto de Investigación en Agrobiotecnología (CIALE), Universidad de Salamanca, Salamanca 37185, Spain (e-mail: jmf@usal.es).

Mark Seyfried is with the USDA Agricultural Research Service Northwest Watershed Research Center, Boise, ID 83702 USA (e-mail: mark.seyfried@ars.usda.gov).

Patrick J. Starks is with the USDA Agricultural Research Service Great Plains Agroclimate and Natural Resources Research Unit, El Reno, OK 73036 USA (e-mail: patrick.starks@usda.gov).

Zhongbo Su is with the ITC Faculty, University of Twente, Enschede 7522, The Netherlands (e-mail: z.su@utwente.nl).

Marc Thibeault is with the Comisión Nacional de Actividades Espaciales, Buenos Aires C1063ACH, Argentina (e-mail: mthibeault@conae.gov.ar).

Jeffrey P. Walker is with the Monash University, Melbourne, VIC 3800, Australia (e-mail: jeff.walker@monash.edu.au).

REFERENCES

- [1] D. Entekhabi *et al.*, "The soil moisture active passive (SMAP) mission," *Proc. IEEE*, vol. 98, no. 5, pp. 704–716, May 2010.
- [2] P. O'Neill, E. Njoku, T. Jackson, S. Chan, R. Bindlish, and J. Chaubell, "SMAP algorithm theoretical basis document: Level 2 & 3 soil moisture (passive) data products," Revision F, Jet Propulsion Lab., California Inst. Technol., Pasadena, CA, USA, Tech. Rep. JPL D-66480, 2020.
- [3] M. J. Chaubell *et al.*, "Improved SMAP dual-channel algorithm for the retrieval of soil moisture," *IEEE Trans. Geosci. Remote Sens.*, vol. 58, no. 6, pp. 3894–3905, Jun. 2020, [Online]. Available: <https://doi.org/10.1109/tgrs.2019.2959239>
- [4] A. Colliander *et al.*, "Validation of soil moisture data products from the NASA SMAP mission," 2021.
- [5] A. G. Konings, M. Piles, N. Das, and D. Entekhabi, "L-band vegetation optical depth and effective scattering albedo estimation from SMAP," *Remote Sens. Environ.*, vol. 198, pp. 460–470, 2017.
- [6] Y. H. Kerr *et al.*, "The SMOS mission: New tool for monitoring key elements of the global water cycle," *Proc. IEEE*, vol. 98, no. 5, pp. 666–687, May 2010.
- [7] H. Lawrence *et al.*, "Comparison between SMOS vegetation optical depth products and MODIS vegetation indices over crop zones of the USA," *Remote Sens. Environ.*, vol. 140, pp. 396–406, 2014.
- [8] N. J. Rodríguez-Fernández *et al.*, "An evaluation of SMOS L-band vegetation optical depth (L-VOD) data sets: High sensitivity of L-VOD to above-ground biomass in Africa," *Biogeosciences*, vol. 15, pp. 4627–4645, 2018, [Online]. Available: <https://doi.org/10.5194/bg-15-4627-2018>
- [9] J. P. Grant *et al.*, "Comparison of SMOS and AMSR-E vegetation optical depth to four MODIS-based vegetation indices," *Remote Sens. Environ.*, vol. 172, pp. 87–100, 2016.
- [10] R. Fernandez-Moran *et al.*, "SMOS-IC: An alternative SMOS soil moisture and vegetation optical depth product," *Remote Sens.*, vol. 9, 2017, Art. no. 457.
- [11] T. Mo, B. Choudhury, T. Schmugge, J. Wang, and T. Jackson, "A model for microwave emission from vegetation-covered fields," *J. Geophys. Res., Oceans*, vol. 87, no. C13, 1982, pp. 11229–11237.
- [12] P. E. O'Neill, S. Chan, E. G. Njoku, T. Jackson, R. Bindlish, and J. Chaubell, "SMAP enhanced L2 radiometer half-orbit 9 Km EASE-grid soil moisture, Version 4," NASA Nat. Snow Ice Data Center Distrib. Active Archive Center, Boulder, CO USA, 2020, [Online]. Available: <https://doi.org/10.5067/Q8J8E3A89923>
- [13] M. Simard, N. Pinto, J. Fisher, and A. Baccini, "Mapping forest canopy height globally with spaceborne lidar," *J. Geophys. Res.*, vol. 116, no. 12, 2011, Art. no. G04021.
- [14] V. Avitabile *et al.*, "An integrated pan-tropicat biomass map using multiple reference datasets," *Global Change Biol.*, vol. 22, no. 4, pp. 1406–1420, Oct. 2016.
- [15] A. Colliander *et al.*, "Validation of SMAP surface soil moisture products with core validation sites," *Remote Sens. Environ.*, vol. 191, pp. 215–231, Mar. 2017.
- [16] G. L. Schaefer, M. H. Cosh, and T. J. Jackson, "The USDA natural resources conservation service soil climate analysis network (SCAN)," *J. Atmos. Technol.*, vol. 24, no. 12, 2007, pp. 2073–2077. [Online]. Available: <https://doi.org/10.1175/2007JTECHA930.1>
- [17] H. J. Diamond *et al.*, "U.S. Climate reference network, after one decade of operations: Status and assessment," *Bull. Amer. Meteorol. Soc.*, vol. 94, pp. 485–498, 2013, [Online]. Available: <https://doi.org/10.1175/BAMS-D-12-00170.1>
- [18] B. G. Illston *et al.*, "Mesoscale monitoring of soil moisture across a statewide network," *J. Atmos. Technol.*, vol. 25, pp. 167–182, 2008.
- [19] A. B. Smith *et al.*, "The murrumbidgee soil moisture monitoring network data set," *Water Resour. Res.*, vol. 48, 2012, Art. no. W07701.
- [20] E. Tetlock, B. Toth, A. Berg, T. Rowlandson, and J. T. Ambadan, "An 11-year (2007–2017) soil moisture and precipitation dataset from the kenaston network in the Brightwater Creek Basin, Saskatchewan, Canada," *Earth Syst. Sci. Data*, vol. 11, no. 2, pp. 787–796, 2019.
- [21] H. A. Bhuiyan *et al.*, "Assessing SMAP soil moisture scaling and retrieval in the Carman (Canada) study site," *Vadose Zone J.*, vol. 17, no. 1–14, 2018, Art. no. 180132.
- [22] S. Bircher, N. Skou, K. H. Jensen, J. P. Walker, and L. Rasmussen, "A soil moisture and temperature network for SMOS validation in western Denmark," *Hydrol. Earth Syst. Sci.*, vol. 16, pp. 1445–1463, 2012, [Online]. Available: <https://doi.org/10.5194/hess-16-1445-2012>
- [23] J. Martínez-Fernández and A. Ceballos, "Mean soil moisture estimation using temporal stability analysis," *J. Hydrol.*, vol. 312, pp. 28–38, 2005.
- [24] R. van der Velde *et al.*, "Validation of SMAP L2 passive-only soil moisture products using upscaled in situ measurements collected in Twente, The Netherlands," *Hydrol. Earth Syst. Sci.*, vol. 25, pp. 473–495, 2021.
- [25] T. O. Keefer, M. S. Moran, and G. B. Paige, "Long-term meteorological and soil hydrology database, walnut gulch experimental watershed, Arizona, United States," *Water Resour. Res.*, vol. 44, 2008, Art. no. W05S07, [Online]. Available: <https://doi.org/10.1029/2006WR005702>

- [26] D. D. Bosch *et al.*, "Little river experimental watershed database," *Water Resour. Res.*, vol. 43, 2007, Art. no. W09472, [Online]. Available: <https://doi.org/10.1029/2006WR005844>
- [27] M. S. Seyfried, K. A. Lohse, D. Marks, G. N. Flerchinger, F. Pierson, and S. Holbrook, "Reynolds creek experimental watershed and critical zone observatory," *Vadoze Zone J.*, vol. 17, 2018, Art. no. 180129.
- [28] E. Coopersmith, M. H. Cosh, W. A. Petersen, J. H. Prueger, and J. J. Niemeier, "Soil moisture model calibration and validation: An ARS watershed on the South Fork Iowa River," *J. Hydrometeorol.*, vol. 16, pp. 1087–1101, 2015.
- [29] P. J. Starks, J. L. Steiner, and A. J. Stern, "Upper Washita river experimental watersheds: Land cover data sets (1974–2007) for two southwestern Oklahoma agricultural watersheds," *J. Environ. Qual.*, vol. 43, pp. 1310–1318, 2014, [Online]. Available: <https://doi.org/10.2134/jeq2013.07.0292>
- [30] T. G. Caldwell *et al.*, "The Texas soil observation network: A comprehensive soil moisture dataset for remote sensing and land surface model validation," *Vadose Zone J.*, vol. 18, p. 100034, 2019, doi: [10.2136/vzj2019.04.0034](https://doi.org/10.2136/vzj2019.04.0034).



Julian Chaubell received the Bachelor of Science degree in mathematic from the University of Mar del Plata, Buenos Aires, Argentina, in 1997, and the Ph.D. degree in applied and computational mathematics from the California Institute of Technology, Pasadena, CA, USA, in 2004.

His doctoral work focused on Low-Coherence Interferometric Imaging. In April 2004, he was with Jet Propulsion Laboratory (JPL) in Pasadena, as a Postdoctoral Research Associate with the Tracking Systems and Applications Section, where he worked

on the modeling of EM-wave propagation in fully three-dimensional atmospheric refractive index distributions. In April 2007, he was a Permanent Employee with the Radar Science and Engineering section, JPL, where he has been working on the forward modeling of radar and radiometer measurements as well as retrieval of the geophysical quantity from those measurements. He has also been involved in electromagnetic modeling of electrically large aperture systems and structures. He was part of the SMAP Instrument Operations Team and SMAP Radar L1 Subsystem Team. He is currently a part of the SMAP Radiometer L1 Team and SMAP Soil Moisture L2 Team.



Simon Yueh (Fellow, IEEE) received the Ph.D. degree in electrical engineering from the Massachusetts Institute of Technology, Cambridge, MA, USA, in 1991.

He was a Postdoctoral Research Associate with the Massachusetts Institute of Technology, from February to August 1991. In September 1991, he was with the Radar Science and Engineering Section, the Jet Propulsion Laboratory (JPL) and has assumed various engineering and science management responsibilities. He was the Project Scientist of the National

Aeronautics and Space Administration (NASA) Aquarius mission, from January 2012 to September 2013, the Deputy Project Scientist of NASA Soil Moisture Active Passive Mission, from January 2013 to September 2013, and the SMAP Project Scientist since October 2013. He has been the Principal/Co-Investigator of numerous NASA and DOD research projects on remote sensing of ocean salinity, ocean wind, terrestrial snow and soil moisture. He has authored four book chapters and published more than 200 publications and presentations. He was the recipient of the 2014 IEEE GRSS Transaction Prize Paper Award, 2010 IEEE GRSS Transaction Prize Paper Award, 2002 IEEE GRSS Transaction Prize Paper Award, the 2000 Best Paper Award in the IEEE International Geoscience and Remote Symposium 2000, and the 1995 IEEE GRSS Transaction Prize Paper Award for a paper on polarimetric radiometry. He also the recipient of the JPL Lew Allen Award in 1998, JPL Ed Stone Award in 2003, NASA Exceptional Technology Achievement Award in 2014 and NASA Outstanding Public Leadership Medal in 2017. He was an Associate Editor of Radio Science from 2003 to 2007. He is a Member of the American Geophysical Union, the Editor in Chief of the IEEE TRANSACTIONS OF GEOSCIENCE AND REMOTE SENSING, a Member of URSI Commission F.



algorithm development.

R. Scott Dunbar received the B.S. in degree in physics and astronomy from the University of Albany, New York, NY, USA, in 1976, and the Ph.D. degree in physics from Princeton University, Princeton, NJ, USA, in 1980.

He has been with the Jet Propulsion Laboratory since 1981. Over the last 35 years he has contributed to the development of science algorithms for the NSCAT and SeaWinds ocean vector wind scatterometer projects, and since 2009, he has been working on SMAP soil moisture and freeze-thaw



Andreas Colliander (Senior Member, IEEE) received the M.Sc. (Tech.), Lic.Sc. (Tech.), and D.Sc. (Tech.) degrees in electrical engineering from Aalto University, Espoo, Finland, in 2002, 2005, and 2007, respectively.

He is currently a Research Scientist with the Jet Propulsion Laboratory, California Institute of Technology, Pasadena, CA, USA. His research is focused on development of microwave remote sensing techniques. He is currently leading the calibration and validation of the geophysical retrievals of NASA's SMAP mission and developing multi-frequency retrievals for ice sheets and polar atmosphere.



Dara Entekhabi (Fellow, IEEE) received the B.S. degree in 1983 and the M.S. degree in 1988 in geography from Clark University, Worcester, MA, USA, and the Ph.D. degree in 1990 in civil and environmental engineering from the Massachusetts Institute of Technology (MIT), Cambridge, MA, USA.

He is currently a Professor with the Department of Civil and Environmental Engineering and the Department of Earth, Atmospheric and Planetary Sciences, MIT. He is the Science Team lead for the National

Aeronautics and Space Administration's Soil Moisture Active and Passive (SMAP) mission that was launched January 31, 2015. His research includes terrestrial remote sensing, data assimilation, and coupled land-atmosphere systems modeling.

Dr. Entekhabi is also a Fellow of the American Meteorological Society and the American Geophysical Union. He is a Member of the National Academy of Engineering.



Steven K. Chan (Senior Member, IEEE) received the Ph.D. degree in electrical engineering, specializing in electromagnetic wave propagation in random media, from the University of Washington, Seattle, WA, USA, in 1998.

He is currently a Research Scientist with the NASA Jet Propulsion Laboratory, California Institute of Technology, Pasadena, CA, USA. His work in soil moisture retrieval algorithm development encompasses the NASA Aqua/AMSR-E (2002–2011), the JAXA GCOM-W/AMSR2 (2012–present), and

the NASA Soil Moisture Active Passive mission (2015–present). His research interests include microwave remote sensing of soil moisture and vegetation properties and their applications.



Fan Chen received the Ph.D. degree in climatology from the University of North Carolina, Chapel Hill, NC, USA, in 2006.

She is currently a Visiting Scientist with the Hydrology and Remote Sensing Laboratory, ARS, U.S. Department of Agriculture, Beltsville, MD, USA. Her research interests include validation methodology for satellite retrievals of geophysical variables and application of data assimilation techniques to leverage satellite surface soil moisture products in hydrologic predictions.



Xiaolan Xu received the B.Eng. degree from Zhejiang University, Hangzhou, China in 2006, and the M.S. and Ph.D. degrees from the University of Washington, Seattle, in 2008 and 2011, respectively, all in electrical engineering.

In 2012, she was with the Water and Carbon Cycles Group in Jet Propulsion Laboratory (JPL), California Institute of Technology, Pasadena, CA, USA, as a Postdoctoral Research Associate and has been a Scientist since 2014. She is the Lead Developer for Freeze/Thaw algorithm (L2/3-FT products) with Soil

Moisture Active Passive Satellite Mission. Her research interests include theoretical and numerical studies in the random media and application in microwave remote sensing of environment for both active and passive.

Dr. Xu is the recipient of the Union Radio-Scientifique Internationale (URSI) Awards for 2020 Santimay Basu Prize. She is currently a Science Team Member of CYGNSS.



Rajat Bindlish (Senior Member, IEEE) received the B.S. degree from Indian Institute of Technology, Mumbai, India, in 1993, and the M.S. and Ph.D. degrees from The Pennsylvania State University, State College, PA, USA, in 1996 and 2000 respectively, all in civil engineering.

He is currently with NASA Goddard Space Flight Center. Prior to this, he was with USDA Agricultural Research Service, Hydrology and Remote Sensing Laboratory, Beltsville, MD, USA. He is currently working on soil moisture estimation from microwave

sensors and their subsequent application in land surface hydrology. His research interests involve the application of microwave remote sensing in hydrology.

Dr. Bindlish is a Member of American Geophysical Union. He is a Science Team Member of SMAP, NISAR, Aquarius and GCOM-W missions.



Peggy O'Neill (Fellow, IEEE) received the B.S. degree summa cum laude (Hons.) in geography from Northern Illinois University, DeKalb, IL, USA, in 1976, and the M.A. degree in geography from the University of California at Santa Barbara, Santa Barbara, CA, USA, in 1979. She also did Post-graduate work in civil and environmental engineering from Cornell University, Ithaca, NY, USA.

Since 1980, she has been a Research Physical Scientist with the Hydrological Sciences Laboratory at NASA/Goddard Space Flight Center in Greenbelt,

MD, USA, where she conducts research in soil moisture retrieval and land surface hydrology, primarily through microwave remote sensing techniques.

Ms O'Neill has been a recipient of NASA Outstanding Performance and Special Achievement Awards, the Robert H. Goddard Award of Merit, the 2016 Federal Laboratory Consortium Interagency Partnership Group Award, a USDA Certificate of Appreciation, and the 1994 IGARSS Symposium Prize Paper Award (as co-author). She is currently the SMAP Deputy Project Scientist.



Jun Asanuma received the B.Eng., and M.Eng. degrees in civil engineering from the University of Tokyo, Tokyo, Japan, in 1989 and 1991, respectively, and the Ph.D. degree in civil and environmental engineering from Cornell University, Ithaca, NY, USA, in 1996.

After having worked at the Central Research Center of Nippon Koei Co. Ltd, Japan, as a Research Engineer in hydrology, he was with the Department of Civil and Environmental Engineering, Nagaoka University of Technology, Nagaoka, Japan. He was

a Lecturer with Terrestrial Environmental Research Center with the University of Tsukubain 2000. His research interests include land surface hydrology, with emphases on the exchange of mass and energy between the land and the atmosphere through turbulence theories, modeling techniques, and field measurement techniques.



Aaron A. Berg received the B.Sc. and M.Sc. degrees in geography from the University of Lethbridge, Lethbridge, AB, Canada, in 1995 and 1997, respectively, and the M.S. degree in geological Sciences from the University of Texas at Austin, TX, USA in 2001, and the Ph.D. degree in earth system science from the University of California at Irvine, Irvine, CA, USA, in 2003.

Since 2003, he has been with the Department of Geography, Environment and Geomatics, University of Guelph, Guelph, ON, Canada. His research inter-

ests include physical geography, hydrology and remote sensing with research interests focused on the modeling and observation of soil moisture.



David D. Bosch received the Ph.D. degree in hydrology from the University of Arizona, Tucson, AZ, USA, in 1990.

He is currently a Research Hydrologist with the Southeast Watershed Research Laboratory, Agricultural Research Service, Tifton, Georgia, USA. In 1986, he joined the Agricultural Research Service. He leads a watershed research program investigating the impacts of land use on water balance and quality. His research interests include watershed and landscape scale hydrology; agricultural impacts on water quality; hydrologic and solute transport modeling of watershed processes; riparian buffer hydrology and solute transport; and developing new methods for assessing the impact of agricultural chemicals on ground and surface water supplies.

Dr. Bosch has been active in the validation of remotely sensed soil moisture products since 2000.



Todd Caldwell received the B.S. degree in geosciences from the University of New Mexico, Albuquerque, NM, USA, in 1997, and the M.S. and Ph.D. degrees in hydrogeology from the University of Nevada, Reno, NV, USA, in 1999 and 2011, respectively.

He is currently a Research Hydrologist with the U.S. Geological Survey in the Nevada Water Science Center. His research interests include *in situ* soil moisture measurements and scaling, near-surface geophysics, and numerical modeling and parameter

estimation of soil hydraulic properties.



Michael H. Cosh (Senior Member, IEEE) received the Ph.D. degree in civil and environmental engineering from Cornell University, Ithaca, NY, USA, in 2002.

He is currently a Research Hydrologist with the U.S. Department of Agriculture, Agricultural Research Service, Hydrology and Remote Sensing Laboratory, Beltsville, MD, USA. His current research interests include the monitoring of soil moisture from both in situ resources and satellite products.



Chandra Holifield Collins received the Doctorate degree in soil, water, and environmental science from the University of Arizona, Tucson, AZ, USA, in 2006.

She is a Soil Scientist with the USDA-Agricultural Research Service's Southwest Watershed Research Center. Her research interests include image analysis and the use of remote sensing data for agricultural applications, with current focus on operational tools for rangeland management.



Karsten H. Jensen received the M.Sc. and Ph.D. degrees in hydrology from the Technical University of Denmark, Lyngby, Denmark, in 1977 and 1983, respectively.

He is currently a Professor in hydrology with the University of Copenhagen, København, Denmark. He has been PI for a number of major research programs and is currently director of HOBE—the Danish Hydrological Observatory and project leader of two Danida Fellowship Centre research projects in South Africa and India. His current research interests

include integrated hydrological modeling at catchment scale under current and future climate conditions.



José Martínez-Fernández received the B.S. degree in physical geography, the M.S. degree in water science and technology, and the Ph.D. degree in physical geography from the Universidad de Murcia (UM), Murcia, Spain, in 1985, 1991, and 1992, respectively.

He was a Research Fellow (1988–1992) and a Junior Researcher (1992–1994) with the Department of Geography, UM. He was an Assistant Professor in 1995 and an Associate Professor in 1997 with the Department of Geography, Universidad de Salamanca (USAL), where he has been a Professor of Physical

Geography since May 2018. He is currently the Principal Investigator (PI) with the Water Resources Research Group, Instituto Hispano Luso de Investigaciones Agrarias (CIALE), USAL.

Dr. Martínez-Fernández has been a Member of the Spanish National Biodiversity, Earth Sciences and Global Change Programme R&D Projects Selection Committee.



Mark Seyfried received the B.S. degree in soil science from the University of California, Berkely, CA, USA, and the M.S and Ph.D. degrees in soil genesis and soil physics from the University of Florida, FL, USA.

He is currently a research soil scientist with the USDA, Agricultural Research Service in Boise, Idaho. His current research interests include soil moisture dynamics, stream flow generation and carbon cycling in complex terrain. He has worked with remotely sensed soil water data since 1993.



Patrick J. Starks received the B.S. degree in physical geography from the University of Central Arkansas, Conway, AR, USA, in 1979, the M.A. degree in physical geography from the University of Nebraska-Omaha, Omaha, NE, USA, in 1984, and the Ph.D. degree in agronomy from the University of Nebraska-Lincoln, Lincoln, NE, USA, in 1990.

From 1990 to 1992, he was a Postdoctoral Fellow with the Department of Atmospheric Science, University of Missouri, Columbia, MO, USA. Since 1992, he has been with the USDA Agricultural Research Service, as a Research Soil Scientist and is stationed with the Grazinglands Research Laboratory, El Reno, OK, USA. His research interests include of hydrology, soil science, and remote sensing.



Zhongbo Su received the M.Sc. degree in hydrological engineering from IHE Delft Institute for Water Education, Delft, The Netherlands, and the Ph.D. degree in civil engineering from the Ruhr University, Bochum, Germany.

He is currently a Professor of Spatial Hydrology and Water Resources Management, and the Chairman of the Department of Water Resources, Faculty of Geo-Information Science and Earth Observation, University of Twente, Enschede, The Netherlands.

His current research focuses on remote sensing and numerical modeling of land surface processes and interactions with the atmosphere, earth observation of water cycle and applications in climate, ecosystem and water resources studies, as well as monitoring food security and water-related disasters.



Marc Thibeault received the B.Sc. degree in physics from Laval University, Quebec City, QC, Canada in 1982 and the B.Sc. degree in mathematics from the University of Montreal, Montreal, QC, Canada in 1988, the DC. degree in science from the University of Buenos Aires, Buenos Aires, Argentina in 2004.

He is currently the Head of the SAOCOM Project Science Group, a new L-Band mission of the Argentinian Space Agency. His research interests are on soil moisture, polarimetry and other SAR applications.



Jeffrey P. Walker received the B.E. degree in civil and the B.Surveying degree (Hons.), and the Ph.D. degree in water resources engineering from the University of Newcastle, Callaghan, NSW, Australia, in 1995 and 1999, respectively.

His Ph.D. thesis was among the early pioneering research on estimation of root-zone soil moisture from assimilation of remotely sensed surface soil moisture observations. He is currently with NASA Goddard Space Flight Centre, Greenbelt, MD, USA, to implement his soil moisture work globally. In 2001, he was a Lecturer with the Department of Civil and Environmental Engineering, University of Melbourne, where he continued his soil moisture work, including the development of the only Australian airborne capability for simulating newsatellite missions for soilmoisture. In 2010, he was a Professor with the Department of Civil Engineering, Monash University, Clayton, VIC, Australia, where he is continuing this research. He is contributing to soil moisture satellite missions at NASA, ESA, and JAXA, as a Science Team Member for the Soil Moisture Active Passive mission and Cal/val Team member for the Soil Moisture and Ocean Salinity and Global Change Observation Mission–Water, respectively.

Dr. Walker was the recipient of the University Medal from the University of Newcastle, Callaghan, NSW, Australia.